



# Discovery of COVID-19 Protein Inhibitors in Phenolic Acids of *Azadirachta indica* (Neem) using Docking and Pharmacokinetics

Miah Roney<sup>1,2</sup>, AKM Moyeenul Huq<sup>3</sup>, Mohd Fadhlizil Fasihi Mohd Aluwi<sup>1,2,\*</sup>

<sup>1</sup>Faculty of Industrial Sciences and Technology, Universiti Malaysia Pahang Al-Sultan Abdullah, Pahang 26600, Malaysia

<sup>2</sup>Centre for Bio-aromatic Research, Universiti Malaysia Pahang Al-Sultan Abdullah, Pahang 26300, Malaysia

<sup>3</sup>Centre for Drug and Herbal Research, Faculty of Pharmacy, Universiti Kebangsaan Malaysia, Kuala Lumpur 5300, Malaysia

Received 10 March 2024; Received in revised form 1 August 2024

Accepted 2 September 2024; Available online 25 September 2024

## ABSTRACT

COVID-19, a viral infection caused by the coronavirus SARS-CoV-2, is one of the world's most challenging diseases to cure. The fact that COVID-19 does not currently have any pharmaceutical treatments means that a concentrated effort must be made to discover the much-needed remedies for this illness. The most attractive antiviral targets of SARS-CoV-2 are the spike protein and main protease (M<sup>pro</sup>). In this work, sixteen phenolic acids of *Azadirachta indica* were docked into the active site of the spike protein and M<sup>pro</sup>. The resulting compounds were then subjected to pharmacokinetic studies to establish the lead compounds. Based on the results, ferulic acid was found to be a promising candidate for further research into its potential as a SARS-CoV-2 inhibitor due to its positive anticipated pharmacokinetics and pharmacological properties.

**Keywords:** Anti-COVID-19; *Azadirachta indica*; Docking; Phenolic acid; Pharmacokinetics

## 1. Introduction

In December 2019, the novel coronavirus SARS-CoV-2, the virus that causes COVID-19, was first discovered in patients presenting with severe pneumonia in Wuhan, China [1]. The World Health Organization labelled the situation a pandemic

in February 2020; however, unlike its two predecessors, SARS-CoV and MERS-CoV, the new virus has apparently affected many individuals [2]. There were 700 million cases, increasing exponentially worldwide until December 26, 2023, with 6.9 million fatalities [3]. One of the most major issues is the lack of

a specialised COVID-19 medication for this potentially fatal infection. As a result, the repositioning of licensed medications is necessary as a priority in the battle against COVID-19. There are now a few approved medications, and a few vaccinations are available on the market. Furthermore, antiviral treatments have already been shown to be effective against viral enzymes. This is why antiviral medications were among the first treatment methods explored for COVID-19 [4]. Numerous clinical trials have been conducted since January 2020 to investigate antiviral, anti-inflammatory, and anti-malarial medicines for the cure of COVID-19 [5, 6].

Upon infection, the SARS-CoV-2 spike protein attaches to ACE2 on the surface of human cells, spreading through vesicles, infiltrating the body, and causing illness [7]. The pp1a and pp1ab polyproteins encoded by the human coronavirus 229E replication gene regulate all viral reproduction and transcriptional activities. The C-proximal component of pp1ab expression needs (-1) ribosomal frameshifting. Extensive proteolytic processing is used to liberate functional polypeptides from polyproteins, which is predominantly accomplished by 3C-like proteinase (3CL<sup>pro</sup>) [8]. The SARS-CoV-2 virus is thought to be an efficient target of 3CL<sup>pro</sup>, also known as major protein (M<sup>pro</sup>) [9].

Medicinal plants are highly regarded in the field of medical research because they contain a wealth of bioactive substances that may be exploited to cure a wide range of ailments and diseases [10]. Several reviews of natural sources as potential anti-SARS-CoV-2 medicines have been published. The tropical perennial plant *Azadirachta indica* (Neem) has skewed leaves and a sturdy trunk that has insect-repellant characteristics [11]. This plant has yielded a diverse range of chemical substances that are used as antiseptics [12], antivirals [13], antipyretics [14], anti-inflammatory [15], anti-ulcers [16], anti-malarial [17], antifungal [18], and anticancer [19] agents. Liquid extract of neem leaves reduced 100-10,000 of 50% tissue culture

infectious dose (TCID<sub>50</sub>) of dengue virus (DENV) *in-vitro* with the 1.897 mg/ml maximal non-toxic dose [20]. An antiviral experiment demonstrated that the compounds decrease dengue virus serotype 2 (DENV-2) infectivity dose-dependently, with a maximal viral inhibition of 77.7% and 66.2% observed for kaempferol 3-O-b-rutinoside (100 µM) and epicatechin (1000 µM), respectively, with no notable cell damage [10]. Hot and cold aqueous extraction and a hydro-methanolic extraction of *A. indica* leaves inhibited the influenza virus by 92.5% (0.325 mg/ml) [21]. In addition, *A. indica* has also been discovered to exhibit antiviral action *in-vitro* against Vaccinia [22], Chikungunya [23], and measles viruses [24], as well as group-B Cocksackie viruses [25]. It has also been shown to boost antibody levels against the Newcastle disease virus [21]. Furthermore, phenolic acids have indeed been proven to have numerous biological effects, especially anti-inflammatory [26], anti-malarial, antioxidant [27], antiviral [28], and anti-cancer [29] effects. However, in the face of this COVID-19 epidemic, for which no medicine has yet been licensed, it is critical to boost research in the hunt for a viable therapy.

Following that, the goal of this work was to identify therapeutic candidates based on the antiviral activity of phenolic acids from *A. indica* using computational-based methodologies such as molecular docking simulations and pharmacokinetic property analysis. It has been shown that nirmatrelvir, an oral antiviral that targets 3CL<sup>pro</sup> of SARS-CoV-2, is clinically effective against COVID-19. Additionally, oral nirmatrelvir administration has demonstrated a clinical efficacy of 89% in reducing hospitalisation and mortality rates [30]. Nirmatrelvir was used as a reference drug in this investigation since it is a prospective medication for inhibiting COVID-19.

## 2. Methodology

### 2.1 System preparation and docking

Sixteen phenolic acids of *A. indica* were docked into the active site of target proteins using the online CB-Dock software [31, 32]. The compounds were constructed using ChemSketch and saved in mol format. The spike protein and M<sup>pro</sup> were downloaded with the PDB codes 6LZG [33] and 6M0K [34], respectively. The CB-Dock effectively locates the binding region, establishes the centre's size and position, adjusts the docking region's size according to the molecules it receives, and then uses AutoDock Vina version 1.1.2 to dock [35]. A pdb file for the receptor and a mol file for the ligands were entered before docking. Throughout this process, several top cavities were automatically selected and utilised for additional analysis (cavity sorting), with molecular docking performed at each one. The optimal binding site for the query ligand is thought to be the corresponding location, whereas the first conformation is thought to represent the ideal binding posture. After examining the various binding modalities, the docked position with the highest cavity size and first posture AutoDock Vina score was selected for additional testing.

### 2.2 In-silico pharmacokinetics study

The pkCSM online programme (<http://biosig.unimelb.edu.au/pkcsml/>) was used to estimate the pharmacokinetic parameters of the chosen ligands and the reference compound [36]. As representative predictors, molecular characteristics, CYP inhibitors, hERG inhibitors, and hepatotoxicity were chosen.

## 3. Results and Discussion

### 3.1 Docking

Molecular docking is a computer-based approach that helps researchers better understand protein-ligand interactions. This approach suggests the native location, orientation, and conformation of ligands that bind to the protein target's active site [37]. In this study, sixteen phenolic acids from *A.*

*indica* previously covered in the literature were tested against the structural and non-structural proteins of SARS-CoV-2 [38-46].

SARS-CoV-2 is characterised by two groups of proteins: (i) non-structural proteins, such as proteases, 3-chymotrypsin-like protease (3CL<sub>pro</sub>/M<sup>pro</sup>), papain-like protease (PL<sub>pro</sub>), and RNA-dependent RNA polymerase (RdRp), and (ii) structural proteins, such as spike (S), nucleocapsid (N), matrix (M), and envelope (E). Furthermore, the CoV polyprotein encodes two proteases that work together to digest and release translated non-structural proteins, namely 3CL<sub>pro</sub> and PL<sub>pro</sub> [47]. On the other hand, the angiotensin-converting enzyme 2 (ACE2) functions as a functional receptor for the SARS-CoV and SARS-CoV-2 spike proteins [48]. This enzyme is essential to the renin-angiotensin system and plays a major part in vertebrate blood pressure control. Human ACE2 may be polymorphic, and while its mRNA is known to be found in almost every organ, its protein expression is only found in a few specific tissues, such as the kidneys, heart, thyroid, lungs, colon, liver, and bladder [49]. Mainly responsible for cleaving host polyproteins into proteins linked to viral replication, 3CL<sub>pro</sub> is highly conserved within the SARS-CoV-2 family, which includes SARS-CoVs and Middle East respiratory syndrome coronavirus. The borders between nsp1/2, nsp2/3, and nsp3/4 are cut by PL<sub>pro</sub>. It cleaves the polyproteins into nonstructural proteins (Nsps) by interacting with 3CL<sub>pro</sub>. Nucleoside 5'-triphosphate (NTP)-dependent helicase nsp13 catalyses the unwinding of oligonucleotide duplexes into single strands. Since its sequence is conserved across all CoV species, it is also a prime candidate for the development of antiviral medications. For viral replication and transcription, the C-terminal guanine-N7 methyl transferase (nsp14) and N-terminal exoribonuclease of CoV are essential [47].

This work employed blind docking to anticipate the binding location of both structural and non-structural proteins to

identify the particular phenolic acid of *A. indica* as either a competitive or non-competitive anti-COVID-19 chemical. It was shown that all docked chemicals interacted with the target proteins' active sites. The compounds that have been docked exhibit favourable interaction values and noteworthy hydrogen and hydrophobic bonding interactions, as indicated by the docking data. Based on interactions in the target proteins' active sites, bound amino acids, binding energy, and comparison to the reference molecule (Nirmatrelvir), phenolic acids derived from *A. indica* will have therapeutic effects and can act as anti-COVID-19 inhibitors. SARS-CoV-2 3CL<sub>pro</sub>, a crucial enzyme for the viral life cycle, is inhibited by nirmatrelvir. Nirmatrelvir inhibits viral replication by preventing the virus from digesting its polyproteins through 3CL<sub>pro</sub> inhibition. By using X-ray crystallography, the structural foundation for this inhibition has been clarified. This has revealed how nirmatrelvir binds to the protease's active site, which is essential to the enzyme's activity [50, 51]. Ridgway et al. [52] also reported that nirmatrelvir exhibited 95% suppression of the SARS-CoV-2 spike protein.

The reference compound (nirmatrelvir) exhibited a binding energy of -8.0 kcal/mol to the spike protein and was well fitted into the active site of the protein. Nirmatrelvir formed hydrogen bonds with Asp30, Leu445, Gln409, and Asp405. Furthermore, nirmatrelvir was found to interact with Glu37, Tyr453, Lys417, Asn33, Tyr505, Glu406, and Arg403 via

hydrophobic interactions. Nirmatrelvir is also responsible for the formation of ionic (Arg393, Arg403, His94, and Lys417) and  $\pi$ -cation (Arg403) interactions (Fig. 1a). On the other hand, nirmatrelvir showed a binding energy of -8.2 kcal/mol and formed hydrogen bonds with Glu290, Asp197, Thr198, Asp289, and Glu288 in the M<sup>pro</sup> active site. Nirmatrelvir also exhibited hydrophobic interactions with Leu286, Val204, Thr199, Asp197, Leu272, Leu287, Tyr239, and Tyr237, as well as ionic interactions with Lys5 and Arg131 (Fig. 1b).

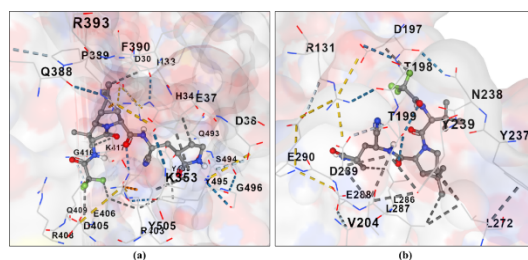


**Fig. 1.** Molecular docking complexes using the CB-Dock software. (a) Structural protein and nirmatrelvir, (b) Non-structural protein and nirmatrelvir.

### 3.1.1 Docking with the structural protein

The binding energies obtained from the docking into the active site of the SARS-CoV-2 spike protein are presented in Tables 1 and 2. Ferulic acid, chlorogenic acid, quercetin, 3,4-dicaffeoylquinic acid, 4,5-di-O-caffeoylquinic acid, and 3,5-di-caffeoylquinic acid showed better binding energy to the active site of spike protein (6LZG) than did the reference compound nirmatrelvir (Table 1).

**Table 1.** Molecular docking results analysis of best phenolic acids and structural protein of SARS-CoV-2 (PDB ID: 6LZG).

Compound Name	Cavity Score	Vina Score (Kcal/mol)	Bound Amino Acids
Ferulic acid	698	-8.3	Gln338, Asp30, Glu35, Ser494, Tyr495, Gly496, Asp38, Glu37, His34 (H-B), Glu37, Tyr495, Tyr453, Lys353, Arg403 (C-H), His34, Arg393, Lys353 (ionic), Arg403 (Pi-cation)
Chlorogenic Acid	698	-8.2	Gln388, Asp30, Glu37, His34, Ser494, Gly496, Lys353, Tyr495 (H-B), Glu37, Lys353, Arg403, Tyr495, Tyr453 (C-H), His34, Arg393, Lys353 (ionic), Arg403 (pi-cation)

Quercetin	698	-8.0	Glu208, Gly205, Ala396, Glu564, Gly561, Glu564 (H-B), Glu208, Leu95, Val209, Ala396 (C-H), Arg219 (ionic), Tyr196 (pi-pi stacking)
3,4-Dicaffeoylquinic acid	698	-9.3	Lys26, Thr92, Gln409, Gln96, Leu455, Asp30, Glu406, Gln388, Glu37, Ser494, Tyr495, Asp38, Gly496 (H-B), Lys26, Leu29, Asp30, Lys417, Tyr453, Pro389, Glu406, His34, Tyr453, Arg403, Tyr495, Glu37, Lys353 (C-H), Arg408, Arg403, His34, Lys417, Arg393, Lys353 (ionic), Arg403 (pi-cation)
4,5-Di-O-caffeoylquinic acid	698	-9.0	Lys26, Gln96, Gln388, Asp38, Glu406, Glu37, Gly496, Asp38, Tyr495, Ser494 (H-B), Lys26, Leu29, Asp30, Pro389, Tyr453, His34, Glu37, Tyr505, Arg403, Lys353 (C-H), Lys417, His34, Arg403, Arg393, Lys353 (ionic), Arg403 (pi-cation)
3,5-Di-caffeoylquinic acid	698	-9.0	Thr92, Gln96, Asp30, His34, Glu406, Ser494, Tyr495, Gly496, Glu37, Asp38 (H-B), Lys26, Leu29, Pro389, Tyr453, Arg403, Glu37, Lys353 (C-H), Arg393, His34, Lys417, Arg403 (ionic), Arg403 (pi-cation)
Nirmatrelvir	698	-8.0	Asp30, Leu445, Gln409, Asp405 (H-B), Glu37, Tyr453, Lys417, Asn33, Tyr505, Glu406, Arg403 (C-H), Arg403 (pi-cation), Arg393, Arg403, His94, Lys417 (ionic)

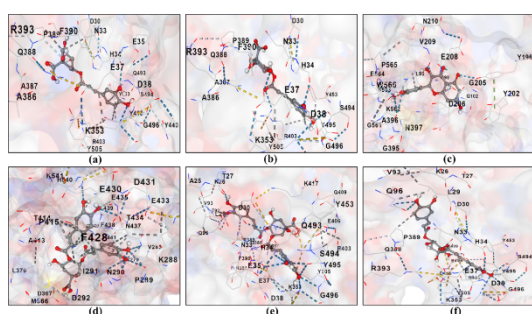


**Fig. 2.** Molecular docking complexes of structural protein and best phenolic acids using the CB-Dock software. (a) Ferulic acid, (b) Chlorogenic acid, (c) Quercetin, (d) 3,4-di-caffeoylquinic acid, (e) 4,5-di-O-caffeoylquinic acid and (f) 3,5-di-caffeoylquinic acid.

Ferulic acid exhibited a binding energy of -8.3 kcal/mol to the spike protein and was well fitted into its active site. Ferulic acid forms hydrogen bonds with Gln338, Asp30, Glu35, Ser494, Tyr495, Gly496, Asp38, Glu37, and His34. Furthermore, ferulic acid was found to interact with Glu37, Tyr495, Tyr453, Lys353, and Arg403 via hydrophobic interactions. Ferulic acid is also responsible for the formation of ionic (His34, Arg393, and Lys353) and  $\pi$ -cation (Arg403) interactions (Fig. 2a).

Chlorogenic acid exhibited a binding energy of -8.2 kcal/mol to the spike protein and was well fitted into the active site of the protein. Chlorogenic acid forms hydrogen bonds with Gln388, Asp30, Glu37, His34, Ser494, Gly496, Lys353, and Tyr495. Furthermore, chlorogenic acid was found to interact with Glu37, Lys353, Arg403, Tyr495, and Tyr453 via hydrophobic interactions. Chlorogenic acid is also responsible for the formation of ionic (His34, Arg393, and Lys353) and  $\pi$ -cation (Arg403) interactions (Fig. 2b).

Quercetin exhibited a binding energy of -8.0 kcal/mol to the spike protein and was well fitted into the active site of the protein. Quercetin forms hydrogen bonds with Glu208, Gly205, Ala396, Glu564, Gly561, and Glu564. Furthermore, quercetin was found to interact with Glu208, Leu95, Val209, and Ala396 via hydrophobic interactions. Quercetin is also responsible for the formation of ionic (Arg219) and  $\pi$ - $\pi$  stacking (Tyr196) interactions (Fig. 2c).

3,4-Dicaffeoylquinic acid exhibited the best binding energy of -9.3 kcal/mol to the spike protein and was well fitted into the active site of the protein. 3,4-Dicaffeoylquinic acid forms hydrogen bonds with Lys26, Thr92,

Gln409, Gln96, Leu455, Asp30, Glu406, Gln388, Glu37, Ser494, Tyr495, Asp38, and Gly496. Furthermore, 3,4-dicaffeoylquinic acid was found to interact with Lys26, Leu29, Asp30, Lys417, Tyr453, Pro389, Glu406, His34, Tyr453, Arg403, Tyr495, Glu37, and Lys353 via hydrophobic interactions. 3,4-dicaffeoylquinic acid is also responsible for the formation of ionic (Arg408, Arg403, His34, Lys417, Arg393, and Lys353) and  $\pi$ -cation (Arg403) interactions (Fig. 2d).

4,5-di-O-caffeoylquinic acid exhibited a binding energy of -9.0 kcal/mol to the spike protein and was well fitted into the active site of the protein. 4,5-di-O-caffeoylquinic acid formed hydrogen bonds with Lys26, Gln96, Gln388, Asp38, Glu406, Glu37, Gly496, Asp38, Tyr495 and Ser494. Furthermore, 4,5-di-O-caffeoylquinic acid was found to interact with Lys26, Leu29, Asp30, Pro389, Tyr453, His34, Glu37, Tyr505, Arg403, and Lys353 via hydrophobic interactions. 4,5-di-O-caffeoylquinic acid is also responsible for the formation of ionic (Lys417, His34, Arg403, Arg393, and Lys353) and  $\pi$ -cation (Arg403) interactions (Fig. 2e).

3,5-di-caffeoylquinic acid exhibited a binding energy of -9.0 kcal/mol to the spike protein and was well fitted into the active site of the protein. 3,5-di-caffeoylquinic acid forms hydrogen bonds with Thr92, Gln96, Asp30, His34, Glu406, Ser494, Tyr495, Gly496, Glu37, and Asp38. Furthermore, 3,5-di-

caffeoylquinic acid was found to interact with Lys26, Leu29, Pro389, Tyr453, Arg403, Glu37, and Lys353 via hydrophobic interactions. 3,5-di-caffeoylquinic acid is also responsible for the formation of ionic (Arg393, His34, Lys417, and Arg403) and  $\pi$ -cation (Arg403) interactions (Fig. 2f).

The chemicals that were chosen had an excellent binding affinity towards the spike protein, with values ranging from -8.0 kcal/mol to -9.3 kcal/mol. Additionally, the findings demonstrated that additional bonds and hydrogen bond formation were involved in the interactions with the target spike protein. Docking position analysis revealed that every chemical was bound in the same binding pocket and that the majority of the bound amino acids were the same for every compound. The docking research indicated that the bound amino acids and binding energy had the greatest influence on the spike protein's inhibition.

### 3.1.2 Docking with non-structural protein

The binding energies obtained from the docking into the active site of the SARS-CoV-2 M<sup>Pro</sup> are presented in Tables 2 and 3. Ferulic acid and 3,5-di-caffeoylquinic acid showed the best binding energy to the active site of M<sup>Pro</sup> (6M0K), higher than that of the reference compound Nirmatrelvir (Table 2).

**Table 2.** Molecular docking results analysis of best phenolic acids and non-structural protein of SARS-CoV-2 (PDB ID: 6M0K).

Compound Name	Cavity Score	Vina Score (Kcal/mol)	Bound Amino Acids
Ferulic acid	390	-7.4	Glu290, Asp289, Asp197, Thr198, Glu288, Leu287, Thr199, Leu271 (H-B), Val204 Thr199, Leu287, Leu286, Leu272, Tyr239 (C-H), Arg131 (ionic)
3,5-di-caffeoylquinic acid	390	-7.4	Asp289, Thr198, Asp197, Thr199, Lys236, Leu271, Leu272 (H-B), Thr199, Asn238, Tyr239, Leu272, Leu287, Tyr237 (C-H), Arg131 (ionic)
Nirmatrelvir	390	-8.2	Glu290, Asp197, Thr198, Asp289, Glu288 (H-B), Leu286, Val204, Thr199, Asp197, Leu272, Leu287, Tyr239, Tyr237 (C-H), Lys5, Arg131 (ionic)

Ferulic acid exhibited a binding energy of -7.4 kcal/mol to the spike protein and was

well fitted into the active site of the protein. Ferulic acid forms hydrogen bonds with



Glu290, Asp289, Asp197, Thr198, Glu288, Leu287, Thr199, and Leu271. Furthermore, ferulic acid was found to interact with Val204, Thr199, Leu287, Leu286, Leu272, and Tyr239 via hydrophobic interactions. Ferulic acid is also responsible for the formation of ionic interactions with Arg131 (Fig. 3a).

3,5-di-caffeoylquinic acid exhibited a binding energy of -7.4 kcal/mol to the spike protein and was well fitted into the active site of the protein. 3,5-di-caffeoylquinic acid formed hydrogen bonds with Asp289, Thr198, Asp197, Thr199, Lys236, Leu271, and Leu272. Furthermore, 3,5-di-caffeoylquinic acid was found to interact with Thr199, Asn238, Tyr239, Leu272, Leu287, and Tyr237 via hydrophobic interactions. 3,5-Di-caffeoylquinic acid is also responsible for the formation of ionic interactions with Arg131 (Fig. 3b).

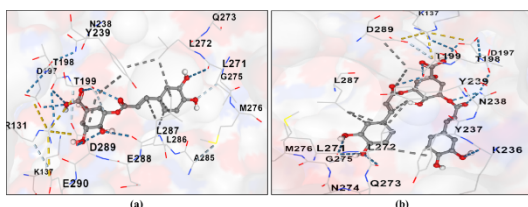


**Fig. 3.** Molecular docking complexes of structural protein and the best phenolic acids using CB-Dock software. (a) Ferulic acid and (b) 3,5-di-caffeoylquinic acid.

The chosen chemicals' binding affinity to the primary protein was similar, at -7.4 kcal/mol. Additionally, the analysis demonstrated that additional bonds and the properties of hydrogen bond formation were involved in the interactions with the target primary protein. Each drug was shown to be bound in the same binding pocket, with the majority of the bound amino acids being the same for every molecule, according to docking position assessments. Docking research revealed that the spike protein was mostly inhibited by bound amino acids and ligand binding.

### 3.2 In-silico Pharmacokinetics Study

The pharmacokinetic profiles of the selected ligands and nirmatrelvir were also computed. The potential for harmful effects of these ligands as medications was assessed using several predictors, such as surface area, hepatotoxicity, CYP inhibition, CYP substrate interaction, human intestinal absorption, blood-brain barrier permeation, and hydrogen bond donor and acceptor. Since the pkCSM programme can create a small-compound pharmacokinetic profile based on a database compilation of QSAR models, it was used as the bioinformatics platform to optimise these characteristics [53]. The outcome of this prediction is displayed in Table 3.

**Table 3.** Pharmacokinetics of selected compounds.

C/N	MW	Log P	H - A	H - D	Surface Area	HIA (% Absorbed)	BB (Log BB)	CYP Substrate	CYP Inhibitor	hERG I inhibitor	Hepatotoxicity	Skin Sensitization
Ferulic acid	194.186	1.4986	3	2	81.065	93.723	-0.252	No	No	No	No	No
Chlorogenic Acid	354.311	-0.6459	8	6	141.587	11.995	1.521	No	No	No	Yes	No
Quercetin	302.238	1.988	7	1	122.108	69.235	1.372	No	No	No	No	No
Epicatechin	290.271	1.5461	6	5	119.662	62.847	1.069	No	No	No	No	No
3,4-Dicaffeoylquinic acid	516.455	1.0296	1	7	209.119	20.4	2.055	No	No	No	No	No
4,5-Di-O-caffeoylquinic acid	516.455	1.0296	1	7	209.119	20.4	2.055	No	No	No	No	No

3,5-Di- caffeoylquinic acid	516.4 55	1.02 96	1 1	7	209.1 19	28.715	- 2.06 3	No	No	No	No	No
Nirmatrelvir	499.5 34	1.09 71	5	3	201.6 95	65.723	- 0.94 9	No	No	No	Yes	No

Molecular Weight: molecular weight  $\leq 500$

LogP: partition coefficient  $\leq 5$

Hydrogen Bond Acceptor: number of hydrogens acceptor  $\leq 10$

Hydrogen Bond Donor: number of hydrogen donor  $\leq 5$

Surface Area:  $>150$ : very low absorption

Human Intestinal Absorption: A value between 0 and 20% indicates poor absorption, 20–70% shows moderate absorption, and 70–100% indicates good absorption

Blood Brain Barrier: A value  $>0.1$  indicates low absorption, 0.1–2.0 shows middle absorption, and  $>2.0$  shows higher absorption

CYP Substrate: No

CYP Inhibitor: No

hERG Inhibitor: No

Hepatotoxicity: No

Skin Sensitization: No

The drug-likeness of each selected compound from the docking experiments was assessed using Lipinski's Ro5. According to Ro5, medicines should have a maximum molecular weight of 500 Da, a maximum HBD and HBA of 5 and 10, respectively, a maximum logP of 5, and a maximum surface area of  $150 \text{ \AA}^2$ . It appeared that only ferulic acid met these requirements and passed the Ro5 evaluation. These results suggested that ferulic acid was a drug-like molecule and a good pharmaceutical candidate that could be taken orally.

Cytochrome P450 (CYP450) is a vital enzyme in humans that is responsible for the biotransformation of several xenobiotics. There are more than fifty isoforms and inhibitors in this family of enzymes; however, they also metabolise about 90% of medications. CYP1A2, CYP2C9, CYP2C19, CYP2D6, CYP3A4, and CYP3A5 are usually considered to be the most significant of the CYP450 enzymes [53]. To find out if a drug might interact with another medication in the body and have insufficient pharmacological effect or if toxicities could occur, it is essential to profile the drug candidate interactions with these enzymes [54]. In the present study, it was revealed that none of the selected ligands interact with CYP450, either as a substrate or an inhibitor.

The human ether-à-go-go-related gene (hERG) produces a potassium ion receptor that repolarizes the cardiac action

potential to contribute to electrical heart activity [55]. Drugs that block this channel may cause arrhythmia, or irregular heartbeat, which may result in symptoms that are potentially fatal. None of the three ligands that the hERG inhibitor predictor evaluated was able to block this channel, which suggests that they might be effective as an alternative treatment. The system was also utilised to forecast the selected ligands' potential for hepatotoxicity. Every ligand was shown to pose no risk for hepatic damage. It was demonstrated that all ligands were appropriate as therapeutic agents for dengue treatment based on their anticipated pharmacological properties. Drug similarity, a subjective concept employed in drug design, characterises a "druglike" set of compounds qualities in terms of factors like bioavailability [56]. Ferulic acid (93.723%) was shown to have good intestinal absorption for humans based on the prediction.

Hepatotoxicity was yet another toxicity metric made available by pkCSM. According to predictions, excluding chlorogenic acid, all compounds have no hepatotoxic characteristics and have no activity relating to liver damage [57]. Notably, the reference compound did show a hepatotoxic profile. Based on the results, ferulic acid followed the criteria of Ro5 and had a favorable pharmacokinetic profile.



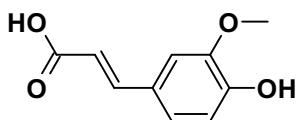


Fig. 4. Structure of lead compound (Ferulic acid).

Ferulic acid, a lead compound, has a molecular weight of 194.186 kDa, and was also found to have a LogP value of 1.4986. Additionally, this molecule was shown to have HBA and HBD values of 2 and 3, respectively. Ferulic acid also showed a surface area of 81.065, a BBB of -0.252, and an HIA of 93.723. However, this substance did not exhibit any hepatotoxicity, cutaneous sensitivity, or CYP substrate interaction or inhibition. Every value fell within the permissible limits.

Ferulic acid (Fig. 4), a phenolic hydroxycinnamic acid prevalent in various plants, has numerous bioactivities, including antibacterial [58], antioxidant [59], anticancer [60], anticoagulant [61], and anti-inflammatory [62] properties. It is also a precursor in the production of other aromatic compounds since it is a component of lignin. Plant viruses have also been proven to be resistant to ferulic acid and its analogues. In 2009, Wang et al. developed a variety of ferulic acid analogues with antiviral activity against plant viruses (such as TMV, pepper virus, tomato virus, potato virus, and maize dwarf mosaic virus) [63]. Ferulic acid was discovered to combat the SARS-CoV-2 membrane protein, which did not violate Lipinski's rule; it was also shown to be a non-inhibitor of CYP450, suggesting that it is properly metabolised by CYP450 [64].

Moreover, ferulic acid has drawn interest because of its possible ability to suppress SARS-CoV-2, the virus that causes COVID-19. Studies demonstrate that it can specifically target M<sup>pro</sup>, the primary protease of SARS-CoV-2, which is essential for the viral life cycle. Numerous ferulic acid derivatives have shown encouraging binding affinities to M<sup>pro</sup>, according to *in-silico* studies, with some of these compounds exhibiting efficacies that are on par with, or even higher than, those of

well-known inhibitors like GC376 and N3 [65]. Furthermore, studies show that certain ferulic acid derivatives can reduce the viral burden by preventing SARS-CoV-2 from replicating *in-vitro* [66]. Ferulic acid has low toxicity and antioxidant qualities, but its bioavailability is still an issue. Therefore, more research on its derivatives is needed to improve pharmacokinetic profiles and maximise therapeutic potential against SARS-CoV-2 [65, 66]. Thus, the development of antiviral medicines that specifically target COVID-19 appears to have a bright future, thanks to ferulic acid and its derivatives.

#### 4. Conclusion

In order to uncover potential hits for treatment of SARS-CoV-2 infections, a computational study using the docking of about sixteen phenolic acids of *A. indica* against the spike protein and M<sup>pro</sup> of COVID-19 was undertaken. The selected compounds from the docking experiments were subjected to further pharmacokinetic studies to obtain the lead molecule. According to *in silico* predictions, ferulic acid had better binding interactions with the active site of spike protein and M<sup>pro</sup> than the reference medication, nirmatrelvir. Furthermore, ferulic acid also demonstrated a favourable pharmacokinetic profile. As a result, molecular dynamics investigations should be carried out to forecast the stability of the ligand-protein complex created during the docking simulation operations. Ferulic acid, with its promising projected pharmacological properties, is an interesting subject for future investigation into developing anti-COVID-19 drugs.

#### References

- [1] Li J, He X, Yuan Y, Zhang W, Li X, Zhang Y, Dong G. Meta-analysis investigating the relationship between clinical features, outcomes, and severity of severe acute respiratory syndrome coronavirus 2 (SARS-CoV-2) pneumonia. *Am J Infect Control* 2021;49(1):82-9.

- [2] Amparo TR, Seibert JB, Silveira BM, Costa FSF, Almeida TC, Braga SFP, de Souza GHB. Brazilian essential oils as source for the discovery of new anti-COVID-19 drug: a review guided by in silico study. *Phytochem Rev* 2021;20(5):1013-32.
- [3] <https://www.worldometers.info/corona-virus/>.
- [4] Ali A, Sepay N, Afzal M, Sepay N, Alarifi A, Shahid M, Ahmad M. Molecular designing, crystal structure determination and in silico screening of copper (II) complexes bearing 8-hydroxyquinoline derivatives as anti-COVID-19. *Bioorg Chem* 2021;110:104772.
- [5] Gasmi A, Peana M, Noor S, Lysiuk R, Menzel A, Gasmi Benahmed A, Bjørklund G. Chloroquine and hydroxychloroquine in the treatment of COVID-19: the never-ending story. *Appl microbiol biotechnol* 2021;105:1333-43.
- [6] Gyselinck I, Janssens W, Verhamme P, Vos R. Rationale for azithromycin in COVID-19: an overview of existing evidence. *BMJ Open Res* 2021;8(1):e000806.
- [7] Meinhardt J, Radke J, Dittmayer C, Franz J, Thomas C, Mothes R, Heppner FL. Olfactory transmucosal SARS-CoV-2 invasion as a port of central nervous system entry in individuals with COVID-19. *Nat neurosci* 2021;24(2):168-75.
- [8] Xu J, Gao L, Liang H, Chen SD. In silico screening of potential anti-COVID-19 bioactive natural constituents from food sources by molecular docking. *Nutri* 2021;82:111049.
- [9] Elmezayen AD, Al-Obaidi A, Şahin AT, Yelekçi K. Drug repurposing for coronavirus (COVID-19): in silico screening of known drugs against coronavirus 3CL hydrolase and protease enzymes. *J Biomol Struct Dyn* 2021;39(8):2980-92.
- [10] Dwivedi VD, Bharadwaj S, Afroz S, Khan N, Ansari MA, Yadava U, Kang SG. Anti-dengue infectivity evaluation of bioflavonoid from *Azadirachta indica* by dengue virus serine protease inhibition. *J Biomol Struct Dyn* 2021;39(4):1417-30.
- [11] Paul R, Prasad M, Sah NK. Anticancer biology of *Azadirachta indica* L (neem): a mini review. *Cancer biol ther* 2021;12(6):467-76.
- [12] Vijayakumar S, Divya M, Vaseeharan B, Ranjan S, Kalaiselvi V, Dasgupta N, Durán-Lara EF. Biogenic preparation and characterization of ZnO nanoparticles from natural polysaccharide *Azadirachta indica* L.(neem gum) and its clinical implications. *J Cluster Sci* 2021;32:983-93.
- [13] Baildya N, Khan AA, Ghosh NN, Dutta T, Chattopadhyay AP. Screening of potential drug from *Azadirachta Indica* (Neem) extracts for SARS-CoV-2: An insight from molecular docking and MD-simulation studies. *J mol struct* 2021;1227:129390.
- [14] Nilima T, Pranali S, Madhura T. Medicinal plant as a source of Antipyretic drug: A Review. *Asian J Pharm Technol* 2021;11(1):84-7.
- [15] Banerjee K, Chatterjee M, Sandur R, Nachimuthu R, Madhyastha H, Thiagarajan P. *Azadirachta indica* A. Juss (Neem) oil topical formulation with liquid crystals ensconcing depot water for anti-inflammatory, wound healing and anti-methicillin resistant *Staphylococcus aureus* activities. *J Drug Del Sci Technol* 2021;64:102563.
- [16] Nesa M, Hosen ME, Khan MAI, Kabir MH, Zaman R. In-vitro antifungal activity of *Azadirachta indica*, *Ocimum tenuiflorum* & *Murraya paniculata* leaf extract against three phytopathogenic fungi. *Am. J Pure Appl Sci* 2021;3(5):113-8.
- [17] Sandhir R, Khurana M, Singhal NK. Potential benefits of phytochemicals from *Azadirachta indica* against neurological

- disorders. *Neurochem Int* 2021; 146: 105023.
- [18] Singh P, Tiwari M. Review on *Azadirachta indica*. *Int. J. Pharma. Life Sci* 2021;2(1 Part A):28-33.
- [19] Akinloye OA, Akinloye DI, Lawal MA, Shittu MT, Metibemu DS. Terpenoids from *Azadirachta indica* are potent inhibitors of Akt: validation of the anticancer potentials in hepatocellular carcinoma in male Wistar rats. *J Food Biochem* 2021;45(1):e13559.
- [20] Parida MM, Upadhyay C, Pandya G, Jana AM. Inhibitory potential of neem (*Azadirachta indica* Juss) leaves on dengue virus type-2 replication. *J ethnopharmacol* 2002;79(2):273-8.
- [21] Sood R, Bhatia S, Bhatnagar H, Gupta V, Kumar M, Dimri U, Swarup D. Phytochemical analysis and in vitro screening of selected Indian medicinal plants for antiviral activity against highly pathogenic avian influenza virus. *Spatula DD* 2013;3(3):81-8.
- [22] Biswas K, Chattopadhyay I, Banerjee RK, Bandyopadhyay U. Biological activities and medicinal properties of neem (*Azadirachta indica*). *Curr sci* 2002;1336-45.
- [23] Sangeetha K, Rajarajan S. In-vitro antiviral activity of Indian medicinal plants to Asian and East Central South African lineage of Chikungunya virus. *Int J Pharm Sci Res* 2015;6(2):692.
- [24] Asif M. Antimicrobial potential of *Azadirachta indica* against pathogenic bacteria and fungi. *J Pharm phytochem* 2012;1(4):78-83.
- [25] Badam L, Joshi SP, Bedekar SS. 'In vitro' antiviral activity of neem (*Azadirachta indica*. A. Juss) leaf extract against group B coxsackieviruses. *J comm dis* 1999;31(2):79-90.
- [26] Righi N, Boumerfeg S, Deghima A, Fernandes PA, Coelho E, Baali F, Baghiani A. Phenolic profile, safety assessment, and anti-inflammatory activity of *Salvia verbenaca* L. *J Ethnopharmacol* 2021;272:113940.
- [27] Nea F, Bitchi MB, Genva M, Ledoux A, Tchinda AT, Damblon C, Fauconnier ML. Phytochemical investigation and biological activities of *Lantana rhodesiensis*. *Mol* 2021;26(4):846.
- [28] van de Sand L, Bormann M, Schmitz Y, Heilingloh CS, Witzke O, Krawczyk A. Antiviral active compounds derived from natural sources against herpes simplex viruses. *Viruses* 2021;13(7):1386.
- [29] de Oliveira Raphaelli C, Azevedo JG, dos Santos Pereira E, Vinholes JR, Camargo TM, Hoffmann JF, Nora L. Phenolic-rich apple extracts have photoprotective and anti-cancer effect in dermal cells. *Phytomed. Plus* 2021;1(4):100112.
- [30] Iketani S, Mohri H, Culbertson B, Hong SJ, Duan Y, Luck MI, Ho DD. Multiple pathways for SARS-CoV-2 resistance to nirmatrelvir. *Nat* 2023;613(7944):558-64.
- [31] Padhi AK, Seal A, Khan JM, Ahamed M, Tripathi T. Unraveling the mechanism of arbidol binding and inhibition of SARS-CoV-2: Insights from atomistic simulations. *Eur J pharmacol* 2021;894:173836.
- [32] Roney M, Singh G, Huq AM, Forid MS, Ishak WMBW, Rullah K, Tajuddin SN. Identification of Pyrazole Derivatives of Usnic Acid as Novel Inhibitor of SARS-CoV-2 Main Protease Through Virtual Screening Approaches. *Mol biotechnol* 2023;1-11.
- [33] Wang Q, Zhang Y, Wu L, Niu S, Song C, Zhang Z, Qi J. Structural and functional basis of SARS-CoV-2 entry by using human ACE2. *Cell* 2020;181(4):894-904.
- [34] Dai W, Zhang B, Jiang XM, Su H, Li J, Zhao Y, Liu H. Structure-based design of antiviral drug candidates targeting the SARS-CoV-2 main protease. *Sci* 2020;368(6497):1331-5.

- [35] Liu Y, Grimm M, Dai WT, Hou MC, Xiao ZX, Cao Y. CB-Dock: A web server for cavity detection-guided protein–ligand blind docking. *Acta Pharmacol Sin* 2020;41(1):138-44.
- [36] Pires DE, Blundell TL, Ascher DB. pkCSM: predicting small-molecule pharmacokinetic and toxicity properties using graph-based signatures. *J med Chem* 2015;58(9):4066-72.
- [37] Bhagat RT, Butle SR, Khobragade DS, Wankhede SB, Prasad CC, Mahure DS, Armarkar AV. Molecular docking in drug discovery. *J Pharm Res Int* 2021;46-58.
- [38] Xuan TD, Tsuzuki E, Hiroyuki T, Mitsuhiro M, Khanh TD, Chung IM. Evaluation on phytotoxicity of neem (*Azadirachta indica*. A. Juss) to crops and weeds. *Crop protec* 2004;23(4):335-45.
- [39] Cristo JS, Matias EF, Figueredo FG, Santos JF, Pereira NL, Junior JG, Coutinho HD. HPLC profile and antibiotic-modifying activity of *Azadirachta indica* A. Juss.(Meliaceae). *Ind crops prod* 2016;94:903-8.
- [40] Patil SS, Deshannavar UB, Ramasamy M, Hegde PG. Modeling and optimisation studies on the ultrasound-assisted extraction of phenolic compounds from *Azadirachta indica*. *Chem Eng Commun* 2022;209(10):1423-38.
- [41] Lakshmi T, Krishnan V, Rajendran R, Madhusudhanan N. *Azadirachta indica*: A herbal panacea in dentistry–An update. *Pharm rev* 2015;9(17):41.
- [42] Stojanović BT, Mitić SS, Stojanović GS, Mitić MN, Kostić DA, Paunović ĐĐ, Pavlović AN. Phenolic profiles and metal ions analyses of pulp and peel of fruits and seeds of quince (*Cydonia oblonga* Mill.). *Food Chem* 2017;232:466-75.
- [43] Narnoliya LK, Sangwan N, Jadaun JS, Bansal S, Sangwan RS. Defining the role of a caffeic acid 3-O-methyltransferase from *Azadirachta indica* fruits in the biosynthesis of ferulic acid through heterologous over-expression in *Ocimum* species and *Withania somnifera*. *Planta* 2021;253:1-13.
- [44] Srivastava S, Srivastava AK. Effect of elicitors and precursors on azadirachtin production in hairy root culture of *Azadirachta indica*. *Appl biochem biotechnol* 2014;172:2286-97.
- [45] Dorababu D, Joshi MC, Kumar BGMM, Chaturvedi A, Goel RK. Effect of aqueous extract of neem (*Azadirachta indica*) leaves on offensive and defensive gastric mucosal factors in rats. *Ind j physiol pharmacol* 2006;50(3):241.
- [46] Mukherjee A, Sengupta S. Characterization of nimbidol as a potent intestinal disaccharidase and glucoamylase inhibitor present in *Azadirachta indica* (neem) useful for the treatment of diabetes. *J enzyme inhibit med chem* 2013;28(5):900-10.
- [47] Hossain R, Sarkar C, Hassan SMH, Khan RA, Arman M, Ray P, Calina D. In silico screening of natural products as potential inhibitors of SARS-CoV-2 using molecular docking simulation. *Chinese j integrat med* 2022;28(3):249-56.
- [48] Li Q, Guan X, Wu P, Wang X, Zhou L, Tong Y, Feng Z. Early transmission dynamics in Wuhan, China, of novel coronavirus–infected pneumonia. *New Eng j med* 2020;382(13):1199-207.
- [49] Rendon-Marin S, Martinez-Gutierrez M, Whittaker GR, Jaimes JA, Ruiz-Saenz J. SARS CoV-2 spike protein in silico interaction with ACE2 receptors from wild and domestic species. *Front Gene* 2021;12:571707.
- [50] Jiang X, Su H, Shang W, Zhou F, Zhang Y, Zhao W, Xu Y. Structure-based development and preclinical evaluation of the SARS-CoV-2 3C-like protease inhibitor simnotrelvir. *Nat Communicat* 2023; 14(1): 6463.
- [51] Lee JT, Yang Q, Gribenko A, Perrin Jr BS, Zhu Y, Cardin R, Hao L. Genetic

- p>surveillance of SARS-CoV-2 Mpro reveals high sequence and structural conservation prior to the introduction of protease inhibitor Paxlovid.
- Mbio*
- 2022;13(4):e00869-22.
- [52] Ridgway H, Moore GJ, Gadanec LK, Zulli A, Apostolopoulos V, Hoffmann W, Matsoukas JM. Novel benzimidazole angiotensin receptor blockers with anti-SARS-CoV-2 activity equipotent to that of nirmatrelvir: computational and enzymatic studies. *Expert Opin Ther Target* 2024;28(5):437-59.
- [53] Roney M, Huq AM, Rullah K, Hamid HA, Imran S, Islam MA, Mohd Aluwi MFF. Virtual screening-based identification of potent DENV-3 RdRp protease inhibitors via in-house usnic acid derivative database. *J Comput Biophys Chem* 2021;20(08)797-814.
- [54] Zhang RX, Dong K, Wang Z, Miao R, Lu W, Wu XY. Nanoparticulate drug delivery strategies to address intestinal cytochrome P450 CYP3A4 metabolism towards personalized medicine. *Pharm* 2021; 13(8): 1261.
- [55] Su S, Sun J, Wang Y, Xu Y. Cardiac hERG K<sup>+</sup> channel as safety and pharmacological target. *Pharmacol potassium chan* 2021;139-66.
- [56] David F, Davis AM, Gossing M, Hayes MA, Romero E, Scott LH, Wigglesworth MJ. A perspective on synthetic biology in drug discovery and development—current impact and future opportunities. *SLAS DISCOVERY: Adv Sci Drug Dis* 2021;26(5):581-603.
- [57] Nishinarizki V, Hardianto A, Gaffar S, Muchtaridi M, Herlina T. Virtual screening campaigns and ADMET evaluation to unlock the potency of flavonoids from *Erythrina* as 3CLpro SARS-COV-2 inhibitors. *J Appl Pharm Sci* 2023;13(2):078-88.
- [58] Borges A, Ferreira C, Saavedra MJ, Simões M. Antibacterial activity and mode of action of ferulic and gallic acids against pathogenic bacteria. *Microb drug resist* 2013;19(4): 256-65.
- [59] Zduńska K, Dana A, Kolodziejczak A, Rotsztejn H. Antioxidant properties of ferulic acid and its possible application. *Skin pharmacol. Physiol* 2018; 31(6):332-6.
- [60] Gao J, Yu H, Guo W, Kong Y, Gu L, Li Q, Wang Y. The anticancer effects of ferulic acid is associated with induction of cell cycle arrest and autophagy in cervical cancer cells. *Cancer Cell Int* 2018;18:1-9.
- [61] Yang ML, Song YM. Synthesis and investigation of water-soluble anticoagulant warfarin/ferulic acid grafted rare earth oxide nanoparticle materials. *Rsc Adv* 2015;5(23):17824-33.
- [62] Yin ZN, Wu WJ, Sun CZ, Liu HF, Chen WB, Zhan QP, Hui WU. Antioxidant and anti-inflammatory capacity of ferulic acid released from wheat bran by solid-state fermentation of *Aspergillus niger*. *Biomed. Environ. Sci* 2019;32(1):11-21.
- [63] Wang Z, Xie D, Gan X, Zeng S, Zhang A, Yin L, Hu D. Synthesis, antiviral activity, and molecular docking study of trans-ferulic acid derivatives containing acylhydrazone moiety. *Bioorg med chem lett* 2017;27(17):4096-100.
- [64] Bhowmik D, Nandi R, Jagadeesan R, Kumar N, Prakash A, Kumar D. Identification of potential inhibitors against SARS-CoV-2 by targeting proteins responsible for envelope formation and virion assembly using docking based virtual screening, and pharmacokinetics approaches. *Infect Gene Evo* 2020;84:104451.
- [65] Antonopoulou I, Sapountzaki E, Rova U, Christakopoulos P. The inhibitory potential of ferulic acid derivatives against the SARS-CoV-2 main protease: molecular docking, molecular dynamics, and ADMET evaluation. *Biomed* 2022;10(8):1787.

- [66] Pasquereau S, Galais M, Bellefroid M, Pachón Angona I, Morot-Bizot S, Ismaili L, Herbein G. Ferulic acid derivatives block coronaviruses HCoV-229E and SARS-CoV-2 replication in vitro. *Sci rep* 2022;12(1):20309.